



Imidazo[1,2-*a*]pyrazine diaryl ureas: Inhibitors of the receptor tyrosine kinase EphB4

Scott A. Mitchell^{a,*}, Mihaela Diana Danca^a, Peter A. Blomgren^a, James W. Darrow^a, Kevin S. Currie^a, Jeffrey E. Kropf^a, Seung H. Lee^a, Steven L. Gallion^b, Jin-Ming Xiong^a, Douglas A. Pippin^d, Robert W. DeSimone^a, David R. Brittelli^a, David C. Eustice^c, Aaron Bourret^e, Melissa Hill-Drzewi^f, Patricia M. Maciejewski^c, Lisa L. Elkin^g

^a Department of Medicinal Chemistry, CGI Pharmaceuticals, Inc., 36 East Industrial Road, Branford, CT 06405, USA

^b Department of Computational Chemistry, CGI Pharmaceuticals, Inc., 36 East Industrial Road, Branford, CT 06405, USA

^c Department of Discovery Biology, CGI Pharmaceuticals, Inc., 36 East Industrial Road, Branford, CT 06405, USA

^d Hit-to-Lead Chemistry, Cephalon, Inc., 145 Brandywine Pkwy, West Chester, PA 19380, USA

^e Developmental and Molecular Pathways, Novartis Institutes of Biomedical Research, 186 Massachusetts Ave., Cambridge, MA 02139, USA

^f High-Throughput Biology, Boehringer Ingelheim Pharmaceuticals, Inc., 900 Ridgebury Road, Ridgefield, CT 06877, USA

^g Lead Discovery, Bristol-Myers Squibb, 5 Research Pkwy, Wallingford, CT 06492, USA

ARTICLE INFO

Article history:

Received 28 August 2009

Revised 1 October 2009

Accepted 5 October 2009

Available online 15 October 2009

Keywords:

Imidazo[1,2-*a*]pyrazine

Small molecule drug discovery

EphB4

VEGFR2

Tie2

Receptor tyrosine kinase

Multiplex kinase inhibitors

Anti-angiogenesis

Diaryl ureas

Kinase inhibitors

ABSTRACT

Inhibition of receptor tyrosine kinases (RTKs) such as vascular endothelial growth factor receptors (VEGFRs) and platelet-derived growth factor receptors (PDGFRs) has been validated by recently launched small molecules Sutent[®] and Nexavar[®], both of which display activities against several angiogenesis-related RTKs. EphB4, a receptor tyrosine kinase (RTK) involved in the processes of embryogenesis and angiogenesis, has been shown to be aberrantly up regulated in many cancer types such as breast, lung, bladder and prostate. We propose that inhibition of EphB4 in addition to other validated RTKs would enhance the anti-angiogenic effect and ultimately result in more pronounced anti-cancer efficacy. Herein we report the discovery and SAR of a novel series of imidazo[1,2-*a*]pyrazine diarylureas that show nanomolar potency for the EphB4 receptor, in addition to potent activity against several other RTKs.

© 2009 Elsevier Ltd. All rights reserved.

The Ephrins represent the largest family of receptor tyrosine kinases (RTKs), of which EphB4 is a member. EphB4 plays an important role in a variety of biological processes such as cell aggregation and migration, neural development, embryogenesis and angiogenesis, and vascular development.¹ EphB4 selectively binds to its endogenous receptor EphB2 to promote cell signaling required for angiogenesis, and has been shown to be profoundly up regulated in numerous cancer types.² Many other RTKs that have been shown to control angiogenesis continue to be targets of drug-discovery efforts, such as VEGFR2, PDGFR β and the angiotensin receptor kinase (Tie2).³ Angiogenesis inhibitors work by controlling the host's ability to sprout new blood vessels into the growing tumor, thus depriving the tumor of sufficient blood supply

and as a result new blood vessels into the growing tumor, thus depriving the tumor of sufficient blood supply and as a result starving it of oxygen and essential nutrients. Attenuating angiogenesis through the inhibition of one or more angiogenic kinases has promise to be an effective chemotherapeutic strategy.⁴

With the approval of Avastin[®] (a monoclonal antibody to VEGF) as front line therapy with other chemotherapeutic agents, the approach of attenuating cancer growth by inhibiting angiogenesis has been clinically validated.⁵ Recently both Nexavar^{®6} and Sutent^{®7} were approved for refractory renal cell carcinoma (rRCC) and gastrointestinal stromal tumors (GIST), respectively, and both represent first-in-class small molecule anti-angiogenic agents. There are numerous small molecules in clinical trials that represent a wave of new cancer drugs that inhibit angiogenesis, oncogenesis, or both.⁸ An example of the latter is XL647 (Exelixis) that has entered phase II trials and inhibits the angiogenesis kinases EphB4

* Corresponding author. Tel.: +1 203 315 1222; fax: +1 203 488 1279.

E-mail address: smitchell@cgipharma.com (S.A. Mitchell).

and VEGFR2 as well as oncogenic kinases EGFR and HER2.⁹ Understanding the differences in inhibition of these various angiogenesis-related kinases is critical to the design of new anti-angiogenic small molecule therapeutics.¹⁰ In addition, the concept of multiplex inhibition will continue to grow as it is ascertained clinically which RTKs are critical for the survival of specific cancer types. In this paper, we describe the discovery and SAR of novel small molecule inhibitors of EphB4 that also inhibit VEGFR2 and the angiopoietin receptor kinase Tie2. Although other EphB4 kinase inhibitors have been reported,^{11,12} the molecules in this report represent a novel class of multiplex kinase angiogenesis inhibitors with a 'triplet' inhibition profile.

At the outset of our EphB4 program we implemented a scaffold-based strategy to identify leads for optimization into potent and selective EphB4 inhibitors. Our initial design strategy utilized the imidazo[1,2-*a*]pyrazine (IP) scaffold **1** (Fig. 1).¹³ Screening of our internal libraries, constructed around scaffold (**1**), resulted in the identification of compound **2**, a 62 nM inhibitor of EphB4. This inhibitor was found to be ATP competitive and >20-fold selective against a series of 22 other kinases (Table 1).¹⁴

We then initiated a medicinal chemistry program to identify the key structural elements required for EphB4 activity in this chemical series. The general synthetic route used to prepare the analogs of **2** is depicted in Figure 2. 6,8-Dibromoimidazo[1,2-*a*]pyrazine **4** is readily prepared on a large scale from commercially available dibromoaminopyrazine **3**.^{15,17}

Selective displacement of the 8-bromine of **4** occurs under thermal conditions with a variety of amines. Suzuki coupling of **5** followed by acylation of **6** with aryl isocyanates provided access to the analogs that are the subject of this Letter.

An SAR analysis of the 4-picolyl portion of **2** revealed that the 4-pyridyl moiety was necessary for optimal activity (Table 2). The 2- and 3-picolyl analogs **9** and **10** lost almost all activity. Moving the

pyridine nitrogen towards (compound **11**) or away from (compound **16**) the IP core reduced activity by 200- and 20-fold, respectively. Together, these data indicate the importance of appropriate positioning of the pyridyl nitrogen atom, suggesting a significant binding interaction with the protein. Consistent with this, removal of the pyridine nitrogen to give the benzyl analog **8** resulted in complete loss of activity, as did saturating the pyridine ring to the piperidine **11**. Smaller amines were also found to be 50–100-fold weaker.

The role of the free NH at the 8-position was investigated and it was shown that the oxygen **19** or N-Me **20** analogs had similar potency, with the NH analog **2** having a slight advantage (Table 3). This highlights the fact that a free NH is not a requirement for potent EphB4 inhibitory activity within this chemical series.

We then investigated the influence of simple substituents in the aryl ring of the urea functionality on EphB4 inhibition (Table 4). The SAR of these analogs clearly demonstrated that *meta*-substitution in the terminal phenyl ring was preferred, with the most potent analogs having lipophilic groups such as CF₃ (**2**), Cl (**31**) and Br (**32**). Similar substitution in either the *ortho*- or *para*-position resulted in significant loss of activity.

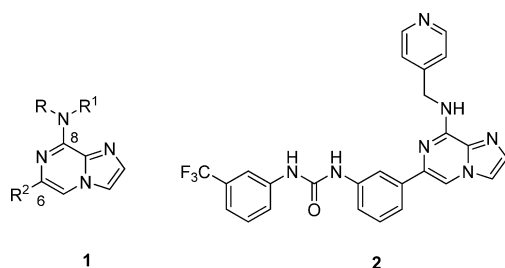


Figure 1. Imidazopyrazine scaffold **1** and EphB4 inhibitor **2**.

Table 1
Biochemical profile of **2**

| Kinase | IC ₅₀ (μM) | Kinase | IC ₅₀ (μM) |
|--------|-----------------------|--------|-----------------------|
| Abl1 | 14.4 | LCK | 50 |
| Akt | 50 | Lyn | 6 |
| Blk | 50 | PDGFRβ | 7.7 |
| Btk | 7.8 | PKA | 50 |
| CDK5 | 50 | PKCa | 50 |
| EGFR | 50 | PKCβ2 | 50 |
| EphA2 | 0.035 | PKCθ | 50 |
| EphB4 | 0.062 | Syk | 50 |
| FGFR4 | 50 | Src | 50 |
| Flt3 | 2 | Tie2 | 0.067 |
| Fyn | 50 | VEGFR1 | 0.747 |
| GSK3b | 50 | VEGFR2 | 0.033 |
| IGFR | 50 | VEGFR3 | 0.071 |
| IRK | 50 | Zap70 | 50 |

All IC₅₀s were obtained at K_m [ATP].

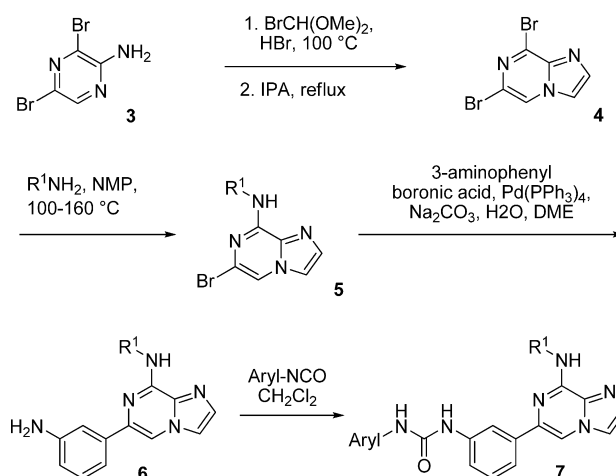


Figure 2. Synthesis of IP-based EphB4 inhibitors.

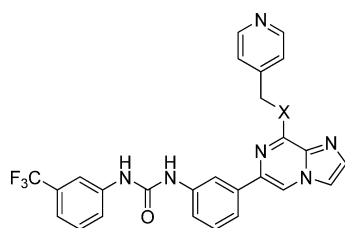
Table 2
Substitution of the aniline group

| Compds | R | EphB4 IC ₅₀ (μM) |
|-----------|--------------------------------------------------------|-----------------------------|
| 2 | CH ₂ -4-pyridine | 0.062 |
| 8 | Benzyl | 50 |
| 9 | CH ₂ -2-pyridine | 32 ^b |
| 10 | CH ₂ -3-pyridine | 7.8 |
| 11 | CH ₂ -4-piperidine | 50 |
| 12 | 4-Pyridine | 32 ^b |
| 13 | 3-Pyridine | 1 ^a |
| 14 | Phenyl | 36 ^b |
| 15 | Methyl | 5.7 ^c |
| 16 | H | 5.4 ^c |
| 17 | CH ₂ CH ₂ -4-pyridine | 0.158 |
| 18 | CH ₂ -4-C ₆ H ₄ -COOH | 5.3 |

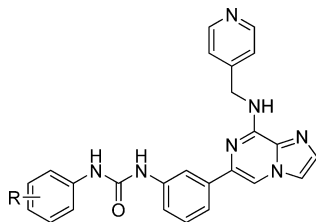
^a % inhibition at 1 μM.

^b % inhibition at 10 μM.

^c 2-OMe-5-Cl instead of 3-CF₃ phenylurea substitution.

Table 3
Variation of linker group

| Compds | X | EphB4 IC ₅₀ (μM) |
|-----------|------|-----------------------------|
| 2 | NH | 0.062 |
| 19 | O | 0.105 |
| 20 | N-Me | 0.069 |

Table 4
SAR of urea: mono-substitution

| Compds | R | EphB4 IC ₅₀ (μM) |
|-----------|-------------------|-----------------------------|
| 2 | 3-CF ₃ | 0.062 |
| 21 | H | 10 ^a |
| 22 | 2-F | 22 ^a |
| 23 | 2-Cl | 2.9 |
| 24 | 2-Br | 1.7 |
| 25 | 2-Me | 30 ^a |
| 26 | 2-OMe | 54 ^a |
| 27 | 2-CF ₃ | 41 ^a |
| 28 | 2-SMe | 63 ^a |
| 29 | 2-OPh | 22 ^a |
| 30 | 3-F | 47 ^a |
| 31 | 3-Cl | 0.165 |
| 32 | 3-Br | 0.213 |
| 33 | 3-Me | 0.3 |
| 34 | 3-OMe | 1.7 |
| 35 | 3-SMe | 1.2 |
| 36 | 3-CN | 1.9 |
| 37 | 3-OPh | 10.5 |
| 38 | 4-Et | 10 ^a |
| 39 | 4-F | 7.4 |
| 40 | 4-Cl | 4.6 |
| 41 | 4-Br | 22 ^a |
| 42 | 4-Me | 7.9 |
| 43 | 4-OMe | 10 ^a |
| 44 | 4-CF ₃ | 10 ^a |

^a % inhibition at 1 μM.

Having established that *meta*-substitution of the phenyl urea was desirable, we then investigated a series of di-substituted (Table 5) and tri-substituted (Table 6) phenyl ureas to see if there were any other substitution patterns that could enhance the potency against EphB4. It was quickly determined that a 2,5-disubstitution pattern of the phenyl urea was advantageous, highlighted by analogs **45–47** and **59–60**. Ureas with groups only in the 2-position were inactive but several groups were tolerated in the 2-position, including F, Cl, Me and OMe, when matched with either a Me, Cl, Br or CF₃ moiety in the 5-position. Other di-substitution patterns were found to have dramatically attenuated activity. This high-

Table 5
SAR of urea: di-substitution

| Compds | Position/R | EphB4 IC ₅₀ (μM) |
|-----------|-------------------------|-----------------------------|
| 45 | 2-OMe-5-CF ₃ | 0.037 |
| 46 | 2-F-5-CF ₃ | 0.053 |
| 47 | 2-Cl-5-CF ₃ | 0.066 |
| 48 | 2,5-Di-Me | 0.938 |
| 49 | 2,5-Di-Cl | 0.101 |
| 50 | 2-OH-5-CF ₃ | 0.037 |
| 51 | 2,3-Di-Cl | 5.7 |
| 52 | 2,4-Di-Cl | 1.9 |
| 53 | 3,4-Di-Cl | 2.5 |
| 54 | 3,5-Di-Cl | 1.8 |
| 55 | 2,6-Di-Cl | 1 |
| 56 | 2-OMe-5-Cl | 0.077 |
| 57 | 2-OPh-5-Cl | 0.138 |
| 58 | 2-Me-5-Cl | 0.16 |
| 59 | 2-OMe-5-Br | 0.026 |
| 60 | 2-OMe-5-Me | 0.078 |
| 61 | 2-OMe-5-CN | 0.125 |
| 62 | 3-CF ₃ -4-Me | 0.81 |
| 63 | 3-CF ₃ -4-F | 0.85 |
| 64 | 3-CF ₃ -4-Cl | 1.2 |

^a % inhibition at [μM].**Table 6**
SAR of urea: tri-substitution

| Compds | Position/R | EphB4 IC ₅₀ (μM) |
|-----------|---------------------------|-----------------------------|
| 65 | 2,4-OMe-5-Cl | 0.402 |
| 66 | 2,4-OMe-5-Br | 0.206 |
| 67 | 2,4-OMe-5-CF ₃ | 0.518 |
| 68 | 2,4-OEt-5-CF ₃ | 0.211 |
| 69 | 2,4,5-Tri-Cl | 0.517 |

lights the fact that 2-substitution in the phenyl urea is only tolerated when accompanied by a suitable group in the 5-position, which corresponds to the *meta*-substitution of the original lead **2**.

We found that trisubstitution of the urea phenyl significantly reduced EphB4 activity, even when the preferred 2,5-disubstitution pattern was embedded. Due to the significant loss in EphB4 activity with compounds substituted in the 4-position, exemplified by 3,4-disubstituted analogs **62–64**, it was not surprising that these tri-substituted analogs had somewhat attenuated potency. Thus, desirable substitution in the phenyl urea was found to be a 2,5 pattern, with a 2-position ranking of OMe > F > Cl and a 5-position ranking of Br ~ CF₃ > Cl.

We then turned to the urea group and investigated its role in EphB4 binding (Table 7). It was found that the urea was optimal in the 3-position of the aryl ring as in **2**, and completely inactive when moved to the 4-position as in **78**. The benzamide **70** and sulfonamide **73** derivatives were significantly less active than the urea **2**. It is clear that proper interaction of the urea functionality with the protein is critical for potent inhibition of EphB4 (Fig. 3).

Compound **2** was docked into a homology model of EphB4 to rationalize the SAR in terms of intermolecular interactions. The pyridine N participates in a H-bond with the amide NH of Met-696. The urea of the inhibitor participates in hydrogen bonds with the side-chains of Lys-647, Asn-745 and Asp-758. The 3-trifluorophenyl is positioned in a mostly hydrophobic pocket formed by residues of the P-loop and C-helix.¹⁶

In summary, the identification of a new series of potent EphB4 inhibitors is reported. Several of the most active molecules (**45,46,59**) were also found to have potent activity (<100 nM) against the angiogenesis-related kinases VEGFR2 and Tie2 (Table 8). These analogs were also assessed in cell-based assays and dem-

- the absence of enzyme and inhibition curves are fit to the data using a Logit curve-fitting algorithm. IC₅₀ values are determined from these inhibition curves.
15. (a) Lumma, W.C. EP 0013914, 1980.; (b) Sablayrolles, C.; Bonnet, P. A.; Cros, G.; Chapat, J. P.; Boucard, M. U.S. Patent 5,028,605, 1991.; (c) Bonnet, P. A.; Michel, A.; Laurent, F.; Sablayrolles, C.; Rechencq, E.; Mani, J. C.; Boucard, M.; Chapat, J. P. *J. Med. Chem.* **1992**, 35, 3353; (d) Mitchell, S. A.; DeSimone, R. W.; Darrow, J. W.; Pippin, D. A.; Danca, M. D. PCT Int. Appl. WO 05/019220, 2005.; (e) Currie, K. S.; DeSimone, R. W.; Pippin, D. A.; Darrow, J. W.; Mitchell, S. A. PCT Int. Appl. WO 04/072081, 2004.; (f) DeSimone, R. W.; Pippin, D. A.; Darrow, J. W.; Mitchell, S. A.; Currie, K. S. PCT Int. Appl. WO 04/022562, 2004.
 16. Models were built in part using the Modeler v7.0 module (X) accessed with InsightII (InsightII v.2000, Accelrys, San Diego).
 17. *A typical experimental (preparation of 2).* 6,8-dibromoimidazo[1,2-*a*]pyrazine: A 1-L four-neck round bottomed flask equipped with a temperature probe, mechanical stirrer and reflux condenser was charged with 2-bromo-1,1-diethoxyethane (68.1 g, 346 mmol) and 48% aqueous hydrogen bromide (11.3 mL, 99.2 mmol), and the reaction mixture was heated at reflux for 2 h. The resulting mixture was allowed to cool to 40 °C and solid sodium bicarbonate (8.50 g, 101 mmol) was added in small portions until gas evolution was observed to cease. *Caution:* initial addition of sodium bicarbonate to the warm solution resulted in vigorous gas evolution (foaming). The resulting suspension was filtered into a 1-L four-neck round bottomed flask and the filter cake was washed with isopropanol (200 mL). The flask was equipped with a temperature probe, mechanical stirrer and reflux condenser. 3,5-Dibromopyrazin-2-amine (50.0 g, 198 mmol) was added and the reaction mixture was heated at reflux with vigorous stirring for 16 h. After this time, the suspension was cooled to 0 °C and filtered. The filter cake was washed with cold isopropanol (50 mL), dried under vacuum and added to a 1-L three-neck round bottomed flask equipped with a mechanical stirrer. Water (200 mL) was added and the vigorously stirred suspension was treated portion-wise with solid potassium carbonate (27.4 g, 198 mmol). *Caution:* gas evolution on the addition of potassium carbonate observed. After stirring for 30 min, the resulting precipitate was isolated by filtration and the filter cake washed with water (100 mL) followed by ethanol (50 mL). The filter cake was dried at 50 °C to a constant weight, under vacuum to provide 6,8-dibromoimidazo[1,2-*a*]pyrazine (52.0 g, 94%) as a light yellow solid: ¹H NMR (300 MHz, DMSO-*d*₆) δ 9.02 (s, 1H), 8.23 (s, 1H), 7.90 (s, 1H). 6-Bromo-*N*-(pyridin-4-ylmethyl)imidazo[1,2-*a*]pyrazin-8-amine: A solution of 6,8-dibromoimidazo[1,2-*a*]pyrazine (500 mg, 1.8 mmol) in acetonitrile (5 mL) was treated with of pyridin-4-ylmethanamine (210 mg, 1.99 mmol) and of K₂CO₃ (1.0 g, 7.24 mmol). The resulting suspension was heated to 95 °C for 24 h with stirring, cooled to rt and partitioned between 0.1 N HCl and EtOAc. The aqueous layer was extracted with EtOAc and combined organic extracts were dried over Na₂SO₄. The solvent was removed under reduced pressure and the resulting residue was purified by flash chromatography (10% MeOH in CH₂CH₂) to yield 6-bromo-*N*-(pyridin-4-ylmethyl)imidazo[1,2-*a*]pyrazin-8-amine as a light tan solid, which was used without further purification. 6-(3-Aminophenyl)-*N*-(pyridin-4-ylmethyl)imidazo[1,2-*a*]pyrazin-8-amine: 6-Bromo-*N*-(pyridin-4-ylmethyl)imidazo[1,2-*a*]pyrazin-8-amine (310 mg, 1.03 mmol) was dissolved in dimethoxyethane (8 mL) and the solution degassed with N₂ at rt for 10 min. To the solution was added 3-aminophenylboronic acid (210 mg, 1.24 mmol), Pd²⁺(PPh₃)₄ (115 mg, 0.10 equiv), and 5 mL of 1 N Na₂CO₃ and the reaction heated to 90 °C with stirring for 24 h. The mixture was cooled to rt and partitioned between 10% AcOH and CH₂Cl₂. The aqueous phase is extracted with CH₂Cl₂ and combined extracts were dried over Na₂SO₄. The solvent is removed under reduced pressure and the resulting residue was purified by flash chromatography (1–5% 2 M NH₃/MeOH/CH₂Cl₂) to yield 6-(3-aminophenyl)-*N*-(pyridin-4-ylmethyl)imidazo[1,2-*a*]pyrazin-8-amine. 1-(3-(8-(Pyridin-4-yl methyl amino) imidazo[1,2-*a*]pyrazin-6-yl)phenyl)-3-(trifluoromethyl) phenyl)urea **2**: A mixture of 6-(3-aminophenyl)-*N*-(pyridin-4-ylmethyl)imidazo[1,2-*a*]pyrazin-8-amine (320 mg, 1.012 mmol) and 1.0 equiv 3-trifluoromethylphenylisocyanate (0.142 mL, 1.012 mmol) were dissolved in toluene. The solution was stirred at rt and the reaction was monitored by LC–MS until complete (30 min). Diethyl ether (20 mL) was then added dropwise to precipitate the product. The sample was filtered and vacuum-dried to provide 330 mg (65%) of 1-(3-(8-(pyridin-4-ylmethylamino)imidazo[1,2-*a*]pyrazin-6-yl) phenyl)-3-(3-(trifluoromethyl)phenyl)urea **2** as an off-white solid. LC–MS purity (98%); MS 504.17 (M+H). ¹H NMR (300 MHz, DMSO-*d*₆) δ 9.05 (s, 1H), 8.80 (s, 1H), 8.44 (dd, 2H, *J* = 1.8 Hz, *J* = 4.5 Hz), 8.35 (s, 1H), 8.34 (d, 1H, *J* = 6.6 Hz), 8.11 (br s, 1H), 8.06 (br s, 1H), 7.93 (d, 1H, *J* = 0.9 Hz), 7.50 (m, 6H) 7.30 (m, 3H) 4.77 (d, 2H, *J* = 6.6 Hz). This synthesis is highly representative of all analogs represented in this Letter.